Catalysis Today 157 (2010) 119–124

Contents lists available at ScienceDirect

Catalysis Today

journal homepage: www.elsevier.com/locate/cattod

Fe-modified TiO_2 photocatalysts for the oxidative degradation of recalcitrant water contaminants

C.A. Castro-López, A. Centeno, S.A. Giraldo*

Centro de Investigaciones en Catálisis (CICAT), Escuela de Ingeniería Química, Universidad Industrial de Santander (UIS), Cra. 27 Calle 9, Bucaramanga, Colombia

ARTICLE INFO

Article history:
Available online 7 August 2010

Keywords:
Fe–TiO_2
Photocatalytic oxidation
Hydrothermal synthesis
Water contaminants

ABSTRACT

Fe–TiO_2 with enhanced photocatalytic oxidation activity was synthesized by hydrolysis of titanium butoxide. Sol–gel process leads to less active Fe–TiO_2 particles than bare TiO_2; meanwhile, the hydrothermal synthesis of Fe–TiO_2 seems to promote the stabilization of Fe^{3+} in the TiO_2 structure promoting the photo-oxidation activity of TiO_2 towards the degradation of azo-dyes and the inactivation of *Escherichia coli* (*E. coli*) in water. Photocatalysts were characterized by X-ray diffraction (XRD), diffusive reflectance spectrophotometry (DRS), and N_2 adsorption–desorption. The TiO_2 synthesized by the hydrothermal synthesis reaches the TiO_2 Degussa P-25 photo-oxidation activity towards the degradation of orange II. Furthermore, Fe loading of TiO_2 in hydrothermal synthesis improves remarkably the photoactivity of HT. The comparative performance of the photocatalysts towards the direct photo-oxidation of iodide, the photocatalytic degradation of orange II and the photocatalytic disinfection of water infected with *E. coli* suggested different mechanisms of oxidation: a surface-hole-oxidation mode for hydrothermally synthesized TiO_2 particles and a homogeneous phase oxidation mode promoted by •OH radicals produced in the TiO_2 P25 surface.

1. Introduction

The photocatalytic oxidation is a recently proposed route for the production of drinking water, especially in zones with high solar irradiations and lack of water supplies. In photocatalysis, the capacity of a UV-A-activated photocatalyst, such as TiO_2, to produce highly oxidant radicals is used to efficiently oxidize a wide variety of organic molecules [1,2] and inactivate bacteria [3,4]. These radicals are produced by redox reactions of water and dissolved oxygen with the UV-A photogenerated charged species of TiO_2: the promoted conduction band electron (e^-) and its positive counterpart, the valence band hole (h^+). Among the oxidative radicals produced in TiO_2 illumination, the hydroxyl radical (•OH) is responsible, in most of the cases, for the complete mineralization of the target molecule [5], as well as the complete inactivation of different bacteria [3].

However, the efficiency of TiO_2 is decreased when the UV-A promoted charged species recombinate, and, thus, the possibility to produce •OH is diminished. Transition metals have been proposed as dopants capable of enhancing the photoactivity of the TiO_2 by trapping the e^-–h^+ pair [6,7]. In particular, iron doping increases the •OH production by its capacity to act as h^+ traps, which reduces the recombination [7–12], and, thus, the chance for the e^-–h^+ to form oxidative radicals is improved. In order to modify the TiO_2 with Fe and achieve an increase in the photocatalytic activity, some synthesis methods in liquid phase have been used, such as sol–gel [9,12,13] and hydrothermal synthesis [10,11,14]. Nevertheless, when Fe is oxidized to Fe_2O_3 and embedded in the TiO_2 matrix, its photoactivity decreases because this oxide acts as a recombination center of the photogenerated charges [9], and thus, reducing photoactivity. Moreover, new insights recently found propose that interactions between Ln^{2+} doped TiO_2 or Fe doped TiO_2 and the target molecule may increase the photo-oxidation, such as, the photosensitization of TiO_2 by organic dye molecules [15], and the photo-leaching of Fe from the TiO_2 matrix [16]. Both processes are not related to the mechanism of recombination but increase the photo-oxidation of the target.

In addition, the coexistence of phases in TiO_2 has been suggested to reduce the recombination of the e^-–h^+ pair [17,18]. Anatase phase, with a band gap (E_g) of 3.2 eV, is known as the most photoactive phase in TiO_2. However, an anatase to rutile phase (E_g of 3.0 eV) ratio of 3:1 shows the best photocatalytic activity of the commercial TiO_2 Degussa P-25 [17]. Such a difference in the E_g of the anatase and rutile phases serves as an energy gradient, which conducts the e^- from rutile to anatase, thus, avoiding the recombination. Similarly, a mixed phase TiO_2, constituted of anatase and brookite phases, has a higher performance towards the degradation of 2-chlorophenol than pure anatase TiO_2 [18]. Then, an increase in photoactivity seems to be correlated to the coexistence of phases anatase and rutile [17] or brookite in TiO_2 [19].

* Corresponding author. Tel.: +57 7 6344746; fax: +57 7 6459647.
E-mail address: sgiraldo@uis.edu.co (S.A. Giraldo).

0920-5861/$ – see front matter © 2010 Elsevier B.V. All rights reserved.
doi:10.1016/j.cattod.2010.04.050

Therefore, the photocatalytic activity of the Fe doped TiO_2 photocatalyst is strongly dependent on the crystalline structure and the state of Fe in the oxide matrix.

In this work, TiO_2 photocatalysts modified with Fe^{3+} were prepared using two different synthesis methods, sol–gel and hydrothermal synthesis using titanium butoxide. The physical properties and the photo-oxidation ability of the Fe doped TiO_2 photocatalysts are correlated to elucidate the state of Fe in the matrix. The photocatalytic production of $^{\bullet}OH$ radicals was followed by means of the photocatalytic degradation of orange II (Or-II), an organic azo-dye recalcitrant to conventional degradation treatments [20] and the deactivation of the *Escherichia coli* strain ATCC 11229 used for disinfectant quality tests [21]. Additionally, the oxidative potential of the photogenerated holes was analyzed towards the direct oxidation of iodide to iodine by the photogenerated h^+ [22].

2. Experimental

2.1. Synthesis of Fe–TiO_2 photocatalysts

Two methods were chosen to synthesize Fe–TiO_2 photocatalysts: sol–gel and hydrothermal synthesis. Fe-SG was synthesized by sol–gel synthesis as follows: titanium butoxide ($Ti(O\text{-}But)_4$; 97% Aldrich) was added dropwise to isopropanol (Isop-OH; Merck), as co-solvent, in a molar ratio Isop-OH/$Ti(O\text{-}But)_4$ = 55. Then, an adequate amount of $Fe(NO_3)_3$ was diluted in water and pH was adjusted to 1.5 with HNO_3 (65%, Merck). Fe aqueous solution was added dropwise to the $Ti(O\text{-}But)_4$-Isop-OH solution. The amount of water corresponds to a molar ratio $H_2O/Ti(O\text{-}But)_4$ = 1.5. Fe content was adjusted to a nominal molar percentage of 0.1 (mol%). The formed solution was stirred until gel was formed. Then, the stirring was stopped, and the gel was aged for 72 h, and immediately dried at 70 °C for 4 h. The obtained crystals were grounded in a mortar, and the yellowish powders were calcined at 400 °C for 2 h. Bare TiO_2 sol–gel synthesized, labeled as SG, was obtained as described above without the addition of the Fe salt.

Fe-HT was hydrothermally synthesized by hydrolysis of $Ti(O\text{-}But)_4$ in aqueous media. In this case, $Ti(O\text{-}But)_4$ was added dropwise to Isop-OH, as co-solvent, in a volume ratio Isop-OH/$Ti(O\text{-}But)_4$ = 10. Then, an adequate amount of $Fe(NO_3)_3$ was diluted in water and pH was adjusted to 1.5 with HNO_3. Then, the Fe aqueous solution was added dropwise to the $Ti(O\text{-}But)_4$-Isop-OH solution. The amount of water corresponds to a volume ratio $H_2O/Ti(O\text{-}But)_4$ = 25. The Fe content was nominally adjusted to 0.1 mol%. The latter suspension was hydrothermally treated with water stream in an autoclave at 120 °C and 1980 kPa for 3 h. Then, water was extracted by evaporation and continuous stirring at 70 °C. Finally, the obtained powders were grounded in a mortar. TiO_2 obtained by hydrothermal synthesis, as described above but with no Fe salt addition, was labeled as HT.

All photocatalysts were named as Fe-Y, where Y stands for the synthesis route of the Fe–TiO_2 photocatalyst, SG for sol–gel synthesis, and HT for hydrothermal synthesis. TiO_2 P25 from Evonik, previously known as Degussa, was used for comparison purposes.

2.2. Photocatalyst characterization

To analyze the phase structure of the photocatalysts, DRX patterns were collected using a D-Max IIIB Rigaku system at room temperature from angles 2θ of 2–70°. The diffractometer was operated at 40 kV and 80 mA with a monochromatic Cu Kα radiation.

Specific surface areas of photocatalyst were determined by the BET method. The N_2 adsorption–desorption isotherms were recorded on a Nova 1300 apparatus of Quantachrome.

UV–vis diffusive reflectance spectra (DRS) were recorded on a PerkinElmer 2034RD lambda 35 UV with an integrating sphere P/NC 6951014 using $BaSO_4$ as a blank reference. The energy band gap widths of the samples were determined using the Kubelka–Munk phenomenological theory [23].

2.3. Photocatalytic tests

Photocatalytic activity tests were performed in 50 mL borosilicate glass reactors illuminated in an ATLAS Suntest CPS+ system with external magnetic stirring. Suntest Xenon lamp's spectrum covers wavelengths from 300 to 800 nm, with 7% of the photons in the UV-A region. Irradiation and temperature were controlled at 400 W/m^2 and 35 °C respectively.

2.3.1. Photocatalytic degradation of orange II

The photocatalytic degradation of Or-II was carried out with a 20 ppm Or-II aqueous solution with 0.25 g/L of photocatalyst. This suspension was stirred for 1 h under darkness prior to illumination. Samples were taken every 15 min for 1 h and centrifuged at 3000 rpm for 15 min. The concentration of Or-II in the supernatant was determined with a HP 8453 UV–vis spectrophotometer at maximum wavelength absorption, 486 nm. Blank experiments were carried out to determine possible degradation by photolysis. The adsorption equilibrium concentration, reached after 1 h of stirring under darkness, was used as the initial value for the photodegradation efficiency calculations. To follow the degradation the obtained Or-II concentration data are presented as a relative concentration during testing time: C/C_0, where C stands for the concentration at any given time and C_0 is the initial concentration.

2.3.2. Photocatalytic disinfection of water

E. coli ATCC 11229 was incubated for 10 h in 100 mL of Luria Bertani growth media (1 wt% , Tryptone from Oxoid), 0.5 wt% yeast extract from Oxoid, and 1 wt% NaCl from Merck) under 120 rpm of stirring at 35 ± 2 °C. A 2 mL aliquot was taken from the growth media for centrifugation at 3000 rpm for 15 min. The supernatant was discarded, and cell biomass pellet was washed twice with saline solution (0.85% NaCl); then, the pellet was suspended in sterilized distilled water and added to a 50 mL borosilicate glass reactor for photocatalytic disinfection. The reaction medium consists of 50 mL of an *E. coli* cell suspension with 0.25 g/L of photocatalyst. Samples were taken from the reaction medium every 15 min for 1 h and serially diluted in saline solution. To follow the concentration of survival *E. coli* 10 μL of the dilutions was plated onto plate count agar (Merck) and incubated for 24 h before growth colony counting. *E. coli* concentration data are presented as the average of 3 countings on plates as colony-forming units per mL (CFU/mL) from independent experiments. Initial concentration of *E. coli* was adjusted to $\sim 1 \times 10^7$ CFU/mL. Blank experiments were carried out to determine any possible bactericidal activity under darkness labeled as dark, and the influence of simulated solar light to cause solar disinfection labeled as solar disinfection (SODIS).

2.3.3. Photocatalytic oxidation of iodide

The direct photo-oxidation of iodide (I^-) by TiO_2 photogenerated hole (h^+) to produce iodine (I_2), Eq. (1) [22], was conducted using a 4.5×10^{-3} M solution of KI with 0.25 g/L of photocatalyst. Samples were taken every 20 min for 1 h and centrifuged at 3000 rpm.

$$2I^- + h^+ \rightarrow I_2 \quad (1)$$

The concentration of iodine in the supernatant was followed by complexation of I_2 with a 50 g/L starch suspension and determined by absorption at 620 nm in a UV–vis spectrophotometer.

3. Results and discussion

3.1. Characterization

The XRD patterns of the TiO_2 and the Fe-modified TiO_2 particles are shown in Fig. 1. It can be seen that XRD patterns of all samples show an anatase-characteristic peak at $2\theta = 25.2^\circ$. No correspondent peaks to Fe phases were identified, possibly due to the low Fe concentrations in TiO_2 matrix. The ionic radius of Fe^{3+} and Ti^{4+} is very similar, 0.79 and 0.75 å respectively for a coordination number of 6, thus, iron ions may substitute titanium on the TiO_2 matrix or be located interstitially forming a Fe–TiO_2 solid solution [14]. In hydrothermally synthesized photocatalysts HT and Fe-HT, the main peak of anatase at $2\theta = 25.2^\circ$ overlaps with the diffraction peaks of brookite phase at $2\theta = 25.34^\circ$ and 25.68°, which is usually found when both phases coexist in TiO_2 structure [18]. A characteristic peak of brookite is observed with a small diffraction at $2\theta = 30.2^\circ$ marked as B in Fig. 1. Fe-HT shows a slight distortion of the diffraction peaks indicating a reduction of crystallinity due to the presence of Fe. This result is in accordance with the fact that Fe^{3+} may be inserted in the TiO_2 matrix as a substituent for Ti^{4+} or interstitially located. In SG and Fe-SG cases, the anatase phase is notorious for both samples with a high crystallinity. This high crystallinity of anatase phase is related to a high photocatalytic activity of the TiO_2 [24]. A slight decrease in this crystallinity is observed when modifying SG with Fe, suggesting an insertion of Fe into the TiO_2 framework.

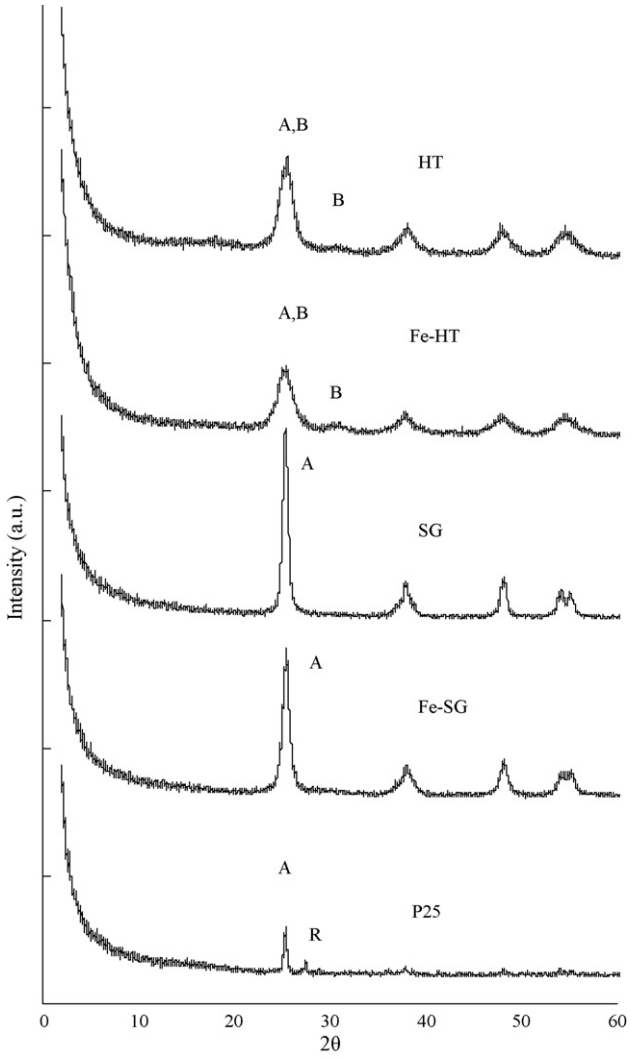

Fig. 1. XRD patterns of TiO_2 (HT, SG, P25) and Fe–TiO_2 (Fe-HT, Fe-SG) samples. A: Anatase, B: Brookite, R: Rutile.

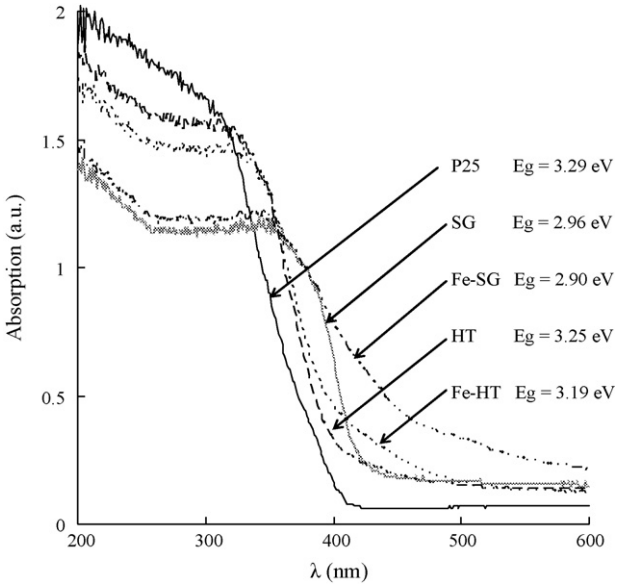

Fig. 2. DRS spectra and their corresponding calculated E_g for the TiO_2 (P25, SG, HT) and Fe–TiO_2 (Fe-SG, Fe-HT) samples.

The DRS spectra of the TiO_2 and Fe–TiO_2 samples and their correspondent energy band gaps (E_g) are shown in Fig. 2. P25 shows the highest absorption in the UV region of the spectrum (200–360 nm), while SG and Fe-SG present the lowest. When comparing the spectrum of bare TiO_2 samples, SG and HT to Fe-modified TiO_2, Fe-SG and Fe-HT, a red-shift is notorious in the absorption to the visible region (>400 nm). Fig. 2 shows the E_g of the photocatalysts obtained by the Kubelka–Munk theory. The reduction in the band gap due to the presence of Fe may be explained since Fe induces new intra band gap states, giving to the TiO_2 the capacity to absorb light at lower energy levels [6], thus, promoting the absorption on the visible part of the spectrum. The excitation of 3d electrons of the Fe^{3+} transferring from the energy level of the dopant to the conduction band of the TiO_2 could effectively shift the absorption threshold into the visible region.

The textural properties, the specific surface area (S_{BET}), and average pore diameter (D_A) of photocatalysts are shown in Table 1. From BET analysis, a decrease is seen in surface area when modifying the TiO_2 with Fe loading in sol–gel (Fe-SG) and hydrothermal synthesis (Fe-HT). Hydrothermal synthesis leads to TiO_2 particles (HT) with higher surface and external area and similar average pore diameter than SG and P25. A decrease in BET area was found when loading TiO_2 with Fe in Fe-HT and Fe-SG cases. Nevertheless, it is important to note that in photocatalysis a higher external area exposed for light absorption is preferred to a higher surface area, since the effective area for photon absorption is the external area of the semiconductor. Thus, for pores hidden to photon absorption no generation of oxidative radicals is expected inside since outer parts of the photocatalyst may screen and scatter light just as when exceeding the concentration of photocatalyst in

Table 1
Textural properties of TiO_2 and Fe-modified TiO_2 samples.

Photocatalyst	HT	Fe-HT	SG	Fe-SG	P25
BET (m^2/g)	161	147	44	41	48
D_A (Å)	17	13	19	N.D.	26

S_{BET}: specific surface area, D_A: average pore diameter, N.D.: not determined.

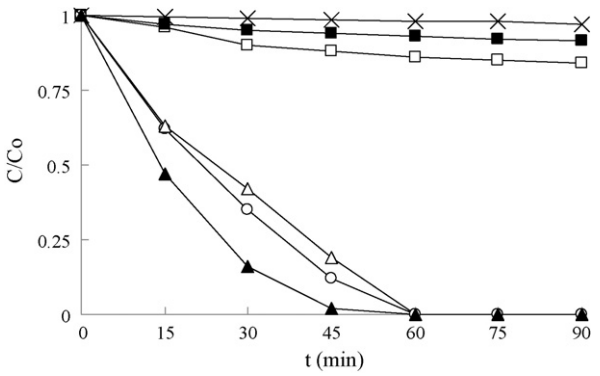

Fig. 3. Or-II degradation as relative concentration C/C_0 by: (■) Fe-SG; (□) SG; (○) P25; (△) HT, and (▲) Fe-HT, during 60 min of 400 W/m^2 of simulated solar light irradiation and (×) blank photolysis.

which light penetration is obstructed [25]. But of course, adsorption of the target molecule may be increased.

3.2. Photocatalytic activity

Fig. 3 shows photocatalytic degradation of Or-II by the TiO_2 and Fe–TiO_2 photocatalysts under simulated solar light irradiation. Sol–gel synthesized samples, SG, and Fe-SG show the lowest performance in the photodegradation of Or-II. This poor photoactivity of sol–gel synthesized samples was not expected by means of crystallinity of the anatase phase since SG has high phase crystallinity. On the other hand, P25, with the lowest crystallinity, shows a high performance. Then, it is not possible to establish a direct relationship between crystallinity of phases and the photoactivity of TiO_2 without comparing the whole set of properties of the samples. In addition, sol–gel synthesized samples showed the lowest absorption capacity in the UV region, which may explain their poor photoactivity (Fig. 2). P25 and HT photocatalysts present almost the same photoactivity. Crystalline structures of each one show two phases. In P25, anatase and rutile are present in a mass ratio of 3–1, and in HT, there exists a combination of anatase and brookite in an undetermined mass ratio. The well-known photoactivity of P25 is ascribed to the coexistence of anatase and rutile [17] due to the difference in the band gap of these phases, which is an energy gradient that forces the rutile photogenerated e^- to an intra band gap energy state of anatase, avoiding its recombination with the h^+ [17]. Therefore, it is possible to assume that the photoactivity of HT may be determined by the synergistic action of the conjunction of phases, anatase and brookite, as suggested by Ardizzone et al. [18].

However, light absorption capacity of HT in the UV region is lower than that of P25 (Fig. 2) suggesting a decrease in photoactivity for HT. This, in fact, seems a contradiction since P25 and HT have similar Or-II phototodegradation activities. The textural properties of the samples may add new clues for comparison purposes. HT particles show a high photoactivity with the highest surface area. Thus, it is expected that HT particles with higher surface area may have even more exposed area for light absorption. In this case, there should be a high possibility for more photons to produce more photogenerated charged species due to a higher surface extension in HT particles, and hence, the reduction in photoactivity caused by the lower light absorption of HT may be compensated and reach the activity of P25. On the other hand, Fe alters the photocatalytic activity of the TiO_2. The concentration of Fe here used is in accordance with the optimal concentrations of Fe in the TiO_2 matrix found by Ghorai et al. [8] and Tong et al. [26]. However, Fe reduces the photoactivity of SG despite the increase in absorption capacity in the visible region as seen in DRS analyses (Fig. 2). Contrarily, there is a remarkable increase in photoactivity in HT due to the presence of Fe in Fe-HT, which indeed promotes visible light absorption. Thus, it is not possible to correlate the photoactivity of Fe-modified TiO_2 particles with the increased visible light absorption capacity. The direct photo-oxidation of iodine may give an explanation of the state of Fe in the TiO_2 network for the photocatalysts. The concentration of iodine reached by the TiO_2 and Fe-modified TiO_2 photocatalysts is shown in Fig. 4. The I_2 concentration reached by the SG sample is slightly higher than its correspondent Fe-modified TiO_2 (Fe-SG), suggesting that Fe is acting as a recombination center for the e^-–h^+ pair. For the Fe-HT sample there is not a significant increase of the performance of HT to suggest the action of Fe as a trap for the h^+. Such trap could avoid the recombination of the photogenerated charges and increase the direct oxidation of I^- to I_2 by the h^+ recombination [22].

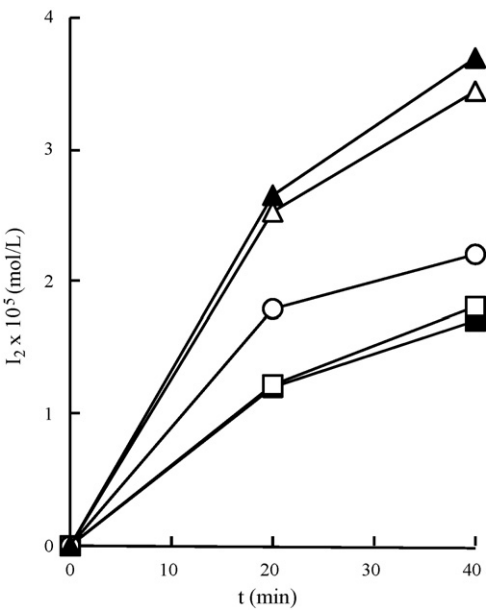

Fig. 4. Concentration of iodine achieved by: (▲) Fe-HT, (△) HT, (○) P25, (□) SG and (■) Fe-SG during 40 min of 400 W/m^2 of simulated solar light irradiation.

Then, it is possible to assume that the chosen sol–gel route promotes Fe as a recombination center for the photogenerated charges in Fe-SG. Meanwhile, the hydrothermal treatment seems to stabilize Fe^{3+} species on the TiO_2 matrix enhancing photoactivity. Fe doping induces some extent deformation on the crystal lattice of the TiO_2 due to the different atomic sizes [26]. However, hydrothermal treatment restrains grain growth, stabilizing particle formation [26], and possibly conducts iron to substitute Ti on the TiO_2 matrix, thus promoting the photoactivity [11].

Adsorption of Or-II molecules on P25 and SG surfaces in the dark agitation period prior to illumination is shorter than adsorption on HT surface indicating a strong interaction of this photocatalyst surface and Or-II. Or-II has a sulfonate functional group ($-SO_3^-$), negatively charged, that promotes its adsorption on positive surfaces [27]. This possibly suggests a direct oxidation of Or-II in the surface of HT and Fe-HT by photogenerated holes; meanwhile P25, with lower Or-II adsorption, may degrade the target molecule by oxidation due to the •OH free radicals in homogeneous phase. This assumption is in agreement with the photo-oxidation of the I^- by the photocatalysts, since HT causes a higher direct oxidation of iodide than P25. Kormali et al. [28] have proposed that oxidation activity of TiO_2 is mainly due to the action of •OH radicals and to a lesser extent to holes. However, the nature of the photo-oxidation mode depends on the nature of the substrate [28]. Additionally, as it is known the e^-–h^+ pair transfer to the media takes 100 ns–1 ms,

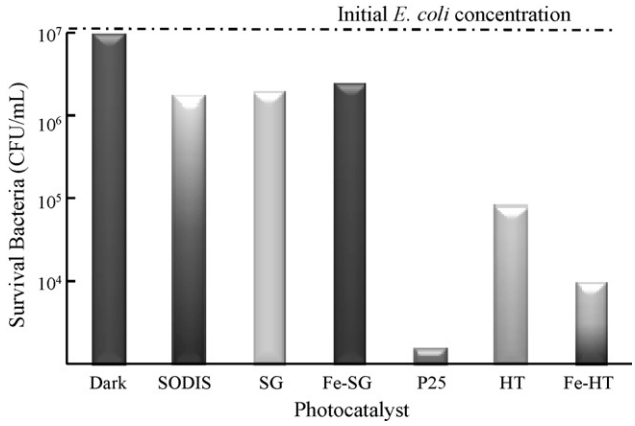

Fig. 5. Survival of *E. coli* ATCC 11229 after 40 min of 400 W/m^2 of simulated solar light irradiation using TiO_2 (SG, P25, HT) and Fe-modified TiO_2 (Fe-SG, Fe-HT) photocatalysts.

and the recombination takes 10–100 ns [2]. Then, it is more probable that surface oxidation by the photogenerated h^+ on the surface of HT takes place faster than the homogeneous phase oxidation caused by •OH homogenous phase free radicals produced on the surface of P25. Indeed, homogeneous phase oxidation of P25 may take additional time for the •OH to reach the Or-II molecules in solution.

The performance of the photocatalyst in the photocatalytic disinfection of water supposes an aggressive test of their photo-oxidation activity, since *E. coli* is a 1–3 μm living cell with protection mechanisms to oxidative stress and 3.5 million macromolecules on its cell wall. The survival bacteria after 40 min of illumination for TiO_2 and Fe-modified TiO_2 photocatalyst are shown in Fig. 5. Blank experiments named as Dark and SODIS indicate no bactericidal activity of the system under darkness and a small disinfection activity of simulated solar light respectively during 40 min of irradiation. The performance of the photocatalysts in the photocatalytic disinfection is comparable to their performance on the Or-II photocatalytic degradation, except for the activity of HT. Unlike the Or-II degradation, the *E. coli* inactivation by HT is lower than that of P25. These results neglect the assumption that HT sample has a similar oxidative power than the one of the P25. Nevertheless, when dealing with enormous complex systems like *E. coli*, compared to 1 nm Or-II molecule, interactions between the target and the photocatalyst become highly important. Gumy et al. [4] found an important relation of the surface charge of the photocatalyst and the cell wall charge. *E. coli* cells have positive and negative charged macromolecules on their surface with predominant negative groups. This implies that a more positive charged surface is preferred to diminish in order to increase the electrostatic attraction between the photocatalyst's surface and bacteria to be efficiently attacked and inactivated.

As proposed before, the oxidation activity of hydrothermally synthesized photocatalysts (HT and Fe-HT) seems to be promoted by surface oxidation due to the h^+. Since Kormali et al. [28] have proposed that the photo-oxidation mode of the photocatalyst depends on the nature of the substrate, and as it is well-known for P25, it is possible that photocatalytic oxidation for the inactivation of *E. coli* in water is mainly caused by the attack of free •OH radicals to the cell wall in the homogenous phase. This assumption on mechanisms may explain the difference in photocatalytic disinfection activities for HT and P25 particles. It is possible to assume that HT particles have a high surface interaction with Or-II to promote surface h^+ oxidation mode, but there is no such interaction between HT surface and *E. coli* to promote a similar •OH radical mode oxidation as P25 do.

Moreover, Fe enhances the photoactivity of the HT sample towards the photocatalytic disinfection of water possibly due to the new interaction bacteria-surface promoted by the presence of Fe. The presence of Fe is not toxic to *E. coli* cells since this element is a macronutrient for microorganisms; thus, the bactericidal activity of the Fe-HT sample is mainly due to photocatalytic reactions. Blank experiments with Fe-HT showed final concentrations of 8.3×10^6 and 8.7×10^6 CFU/mL after 40 min of stirring under darkness, which corroborate the latter assumption.

The photocatalytic disinfection and photocatalytic detoxification activities seem to be related to the crystalline structure, the optical properties, the chemical state of doping metal, and the interactions between the surface of the photocatalyst and the target. In this work we proposed a correlation of these characteristics by comparing the photocatalytic activity of two different Fe–TiO_2 samples synthesized by well-known liquid synthesis methods: sol–gel and hydrothermal synthesis. This correlation allows us to assume that the synthesis route determines the activity of Fe doped TiO_2 since the chosen synthesis may promote the stabilization of Fe in the TiO_2 matrix enhancing the photoactivity. Literature has reported that iron doping in TiO_2 increases photoactivity in the visible region due to the intra band gap states promoted by Fe^{3+} [29], but contrarily, Fe^{3+} may decrease photoactivity [29,30] under UV-light irradiation. These differences in activities may conduct to lower activities under solar light irradiation where both ranges, UV and visible, are used. In this work, we present a feasible synthesis route to obtain Fe doped TiO_2 particles with enhanced photoactivity towards the degradation of the chosen targets under solar light irradiation.

4. Conclusions

Crystalline TiO_2 and Fe-modified TiO_2 particles were synthesized by hydrolysis of titanium butoxide in the presence of a Fe inorganic salt by the sol–gel and the hydrothermal synthesis. Hydrothermal synthesis leads to TiO_2 particles with higher photocatalytic oxidation activity towards the degradation of orange II than TiO_2 sol–gel synthesized particles and similar to the ones of P25. Results of characterization techniques indicate that there is no direct correlation of the photoactivity with the crystallinity of anatase phase but to the presence of amorphous and the coexistence of anatase with one of two phases, rutile and brookite. Fe was effectively inserted in the TiO_2 matrix by the chosen synthesis routes. Diffusive reflectance analysis shows an increase in visible light absorption capacity due to the presence of Fe. However, the sol–gel process promotes Fe as a recombination center of the photogenerated e^-–h^+ reducing photoactivity. Contrarily, hydrothermal synthesis leads to Fe–TiO_2 particles with enhanced photocatalytic activity, possibly due to the stabilization of Fe into the structure at low temperatures.

Additionally, the difference in performance of the photocatalysts when degrading an organic molecule and, on the other hand, inactivating bacteria suggests a difference in mechanisms of photo-oxidation by HT and P25. From analysis of the results, it is possible to assume a surface-hole-oxidation mode for hydrothermally synthesized TiO_2 particles and a homogeneous phase oxidation mode promoted by •OH radicals produced in the TiO_2 P25 surface.

Acknowledgments

This work was financially supported by COLCIENCIAS and SENA (Project code. 1102341-19419). Camilo Castro also thanks the named Colombian government entities and UIS for the financial support for his PhD study.

References

[1] J.M. Herrman, Heterogeneous photocatalysis: fundamentals and applications to the removal of various types of aqueous pollutants, Catal. Today 53 (1999) 115–129.

[2] O. Carp, C.L. Huisman, A. Reller, Photoinduced reactivity of titanium dioxide, Prog. Solid State Chem. 32 (2004) 33–177.

[3] J. Blanco, P. Fernández, S. Malato, Solar photocatalytic detoxification and disinfection of water: recent overview, J. Sol. Energy Eng. 129 (2007) 4–15.

[4] D. Gumy, C. Morais, P. Bowen, C. Pulgarín, S. Giraldo, R. Hajdu, J. Kiwi, Catalytic activity of commercial TiO_2 powders for the abatement of the bacteria (*E. coli*) under solar simulated light: influence of the isoelectric point, Appl. Catal. B: Environ. 63 (2006) 76–84.

[5] M. Mahalaksmi, S. Vishnu, B. Arabindoo, M. Palanichamy, V. Murugesan, Photocatalytic degradation of aqueous propoxur solution using TiO_2 and Hβ zeolite supported TiO_2, J. Hazard. Mater. 161 (2009) 336–343.

[6] W.Y. Choi, A. Termin, M.R. Hoffmann, The role of metal ion dopants in quantum-sized TiO_2: correlation between photoreactivity and charge carrier recombination dynamics, J. Phys. Chem. 98 (1994) 13669–13679.

[7] M.I. Litter, J.A. Navío, Photocatalytic properties of iron doped-titania semiconductors, J. Photochem. Photobiol. A: Chem. 98 (1996) 171–181.

[8] T.K. Ghorai, S.K. Biswas, P. Pramanik, Photo-oxidation of diferent organic dyes (RB, MO, TB, and BG) using Fe(III)-doped TiO_2 nano photocatalyst prepared by novel chemical method, Appl. Surf. Sci. 254 (2008) 7498–7504.

[9] B. Xin, Z. Ren, P. Wang, J. Liu, L. Jing, H. Fu, Study on the mechanisms of photoinduced carriers separation and recombination for the Fe^{3+}–TiO_2 photocatalysts, Appl. Surf. Sci. 253 (2007) 4390–4395.

[10] M. Asiltürk, F. Sayilkan, E. Arpaç, Effect of Fe^{3+} ion doping to TiO_2 on the photocatalytic degradation of Malachite green dye under UV and vis irradiation, J. Photochem. Photobiol. A: Chem. 203 (2009) 64–71.

[11] M.A. Khan, S.I. Woo, O. Yang, Hydrothermally stabilized Fe(III) doped titania active under visible light for water splitting reaction, Int. J. Hydrogen Energy 33 (2008) 5345–5351.

[12] S. Liu, Y. Chen, Enhanced photocatalytic activity of TiO_2 powders doped by Fe unevenly, Catal. Commun. 10 (2009) 894–899.

[13] C.C. Trapalis, P. Keivanidis, G. Kordas, M. Zaharescu, M. Crisan, A. Szatnayi, M. Gartner, TiO_2 (Fe^{3+}) nanostructured thin films with antibacterial properties, Thin Solid Films 433 (2003) 186–190.

[14] C.Y. Wang, C. Bottcher, D.W. Bahneman, J.K. Dohrman, A comparative study of nanometer size Fe(III)-doped TiO_2: photocatalysts: synthesis, characterization and activity, J. Mater. Chem. 13 (2003) 2322–2325.

[15] Y. Xie, C. Yuan, X. Li, Photosensitized and photocatalyzed degradation of azo dye using Ln^{n+}–TiO_2 sol in aqueous solution under visible light irradiation, Mater. Sci. Eng. B 117 (2005) 325–333.

[16] C. Adan, A. Martinez, S. Malato, A. Bahamonde, New insights on solar photocatalytic degradation of phenol over Fe–TiO_2 catalysts: photo-complex mechanism of iron lixiviates, Appl. Catal. B: Environ. 93 (2009) 96–105.

[17] D.C. Hurum, A.G. Agrios, K.A. Gray, T. Rajh, M.C. Thurnauer, Explaining the enhanced photocatalytic activity of Degussa P-25 mixed phase oxide TiO_2 using EPR, J. Phys. Chem. 107 (2003) 4545–4549.

[18] S. Ardizzone, C. Bianchi, G. Cappelletti, S. Gialanella, C. Pirola, V. Ragaini, Tailored anatase/brookite nanocrsytalline TiO_2. The optimal particle features for liquid and gas-phase photocatalytic reactions, J. Phys. Chem. C 111 (2007) 13222–13231.

[19] A. Paola, G. Cufalo, M. Addamo, M. Bellardita, R. Campostrini, M. Ischia, R. Ceccato, L. Palmisano, Photocatalytic activity of nanocrystalline TiO_2 (brookite, rutile, and brookite-based) powders prepared by thermohydrolysis of $TiCl_4$ in aqueus chloride solutions, Colloids Surf. A: Physicochem. Eng. Aspects 317 (2008) 366–376.

[20] P. Pitter, J. Chudoba, Biodegradability of Organic Substances in the Aquatic Environment, CRC Press, Boca Raton, 1990.

[21] G.P. Anipsitakis, T.P. Tufano, D. Dionysiou, Chemical and microbial decontamination of pool water using activated potassium peroxymonosulfate, Water Res. 42 (2008) 2899–2910.

[22] C. Karunakaran, P. Anilkumar, Semiconductor-catalyzed solar photo-oxidation of idodide ion, J. Mol. Catal. A: Chem. 265 (2007) 153–158.

[23] N. Todorova, T. Giannakopoulou, G. Romanos, T. Vaimakis, J. Yu, C. Trapalis, Preparation of fluorine-doped TiO_2 photocatalysts with controlled crystalline structure, Int. J. Photoenergy 2008 (2008) 1–9.

[24] K.Y. Jung, S.B. Park, Anatase-hase titania: preparation by embedding silica and photocatalytic activity forthe decomposition of trichloroethylene, J. Photochem. Photobiol. A: Chem. 127 (1999) 117–122.

[25] I.K. Konstantinou, T.A. Albanis, TiO_2-assisted photocatalytic degradation of azo dyes in aqueous solution: kinetic and mechanistic investigations. A review, Appl. Catal. B: Environ. 49 (2004) 1–14.

[26] T. Tong, J. Zhang, B. Tian, F. Chen, D. He, Preparation of Fe^{3+}-doped TiO_2 catalyst by controlled hydrolisis of titanium alcoxide and study on their photocatalytic activity for methyl orange degradation, J. Hazard. Mater. 155 (2008) 572–579.

[27] C. Guillard, H. Lachheb, A. Houas, M. Ksibi, E. Elaloui, J.M. Herrman, Influence of chemical structure of dyes, of pH and inorganic salts on their photocatalytic degradation by TiO_2 comparison of the efficiency of powder and supported TiO_2, J. Photochem. Photobiol. A: Chem. 158 (2003) 27–36.

[28] P. Kormali, T. Triantis, D. Dimotikali, A. Hiskia, E. Papaconstantinou, On the Photo-oxidative behavior of TiO_2 and $PW_{12}O_{40}^{3-}$: OH radicals versus holes, Appl. Catal. B: Environ. 68 (2006) 139–146.

[29] Y. Wu, J. Zhang, L. Xiao, F. Chen, Preparation and characterization of TiO_2 photocatalyst by Fe^{3+} doping together with Au deposition of organic pollutants, Appl. Catal. B: Environ. 88 (2008) 525–532.

[30] Z. Li, W. Shen, W. He, X. Zu, Effect of Fe-doped TiO_2 nanoparticle derived from modified hydrothermal process on the photocatalytic degradation performance on methylene blue, J. Hazard. Mater. 155 (2008) 590–594.